frontiers in Marine Science

ORIGINAL RESEARCH
published: 10 December 2020
doi: 10.3389/fmars.2020.604487

Ultrastructural Features of an Abundant and Ubiquitous Marine Ciliate, *Uronychia binucleata* (Protista, Ciliophora, Euplotida)

Jingyi Dong[1,2], Xinpeng Fan[3], Tengyue Zhang[1,4], Saleh A. Al-Farraj[5], Thorsten Stoeck[2], Honggang Ma[1] and Lifang Li[6]**

[1] Institute of Evolution & Marine Biodiversity, and College of Fisheries, Ocean University of China, Qingdao, China, [2] Ecology Group, University of Kaiserslautern, Kaiserslautern, Germany, [3] School of Life Sciences, East China Normal University, Shanghai, China, [4] Department of Zoology, Comenius University in Bratislava, Bratislava, Slovakia, [5] Zoology Department, College of Science, King Saud University, Riyadh, Saudi Arabia, [6] Marine College, Shandong University, Weihai, China

OPEN ACCESS

Edited by:
Thomas Wilke,
University of Giessen, Germany

Reviewed by:
Gabriela Küppers,
Consejo Nacional de Investigaciones Científicas y Técnicas (CONICET), Argentina
Carolina Bastidas,
Massachusetts Institute of Technology, United States

***Correspondence:**
Lifang Li
qd_liliy@sina.com
Honggang Ma
mahg@ouc.edu.cn

Specialty section:
This article was submitted to Marine Evolutionary Biology, Biogeography and Species Diversity, a section of the journal Frontiers in Marine Science

Received: 09 September 2020
Accepted: 20 November 2020
Published: 10 December 2020

Citation:
Dong J, Fan X, Zhang T, Al-Farraj SA, Stoeck T, Ma H and Li L (2020) Ultrastructural Features of an Abundant and Ubiquitous Marine Ciliate, Uronychia binucleata (Protista, Ciliophora, Euplotida). Front. Mar. Sci. 7:604487. doi: 10.3389/fmars.2020.604487

The ciliate genus *Uronychia* is a marine group with extremely differentiated cortical and ciliary structures. These structures define its unique evolutionary position in the whole subclass Euplotia. However, to date, few data about the ultrastructure of this genus and related taxa is available. In the present work, a dominant species, *Uronychia binucleata*, was investigated using scanning electron microscopy and transmission electron microscopy. The findings are as follows: (i) this species lacks the typical alveolar plate in its cortex, whereas the abundant electron-lucent vesicular structures occurred densely; (ii) the subpellicular microtubules form a triad configuration in the dorsal side, while appearing in a single configuration in the ventral side; (iii) the cortical granules are extrusomes, which represent a kind of mucocyst instead of ampules; (iv) two kinetosomes in different rows of one cirrus are linked by the single longitudinal connection; (v) the undulating membrane is highly developed and their insides and outsides are partially covered by the cortical flap; (vi) the single-membrane-bound pharyngeal disks interposed with microtubular sheets, and are distributed in three distinct zones. This first detailed report about the ultrastructural features of the genus *Uronychia* will be a key to improve the diagnosis and systematics of this widely distributed and ecologically important genus and its family Uronychiidae.

Keywords: ciliates, euplotids, Protista, ultrastructure, *Uronychia*

INTRODUCTION

Ciliated protists (Ciliophora), a large assemblage of unicellular eukaryotes occupying various ecological niches, play different roles of importance in microbial food webs. This makes them valuable organisms on a long list of research fields related to biodiversity, biocomplexity, genetic evolution, and environmental conservation (Hausmann and Bradbury, 1996; Lynn, 2008;

Kchaou et al., 2009; Song et al., 2009; El-Serehy et al., 2012; Wang et al., 2017; Chen et al., 2018; Huang et al., 2018; Hu et al., 2019; Wang et al., 2019; Yan et al., 2019; Gupta et al., 2020; Li et al., 2020; Sheng et al., 2020; Wu et al., 2020). As one of the highly cosmopolitan and diverse groups within ciliated protists, euplotid ciliates have been attracting great interest among ciliate researchers. However, the indications suggest that they have indeterminate biodiversity (Song, 1997; Küppers, 2020; Lian et al., 2020; Mendez-Sanchez et al., 2020). As research is developed and extended, more detailed macroscopic and microscopic characteristics are crucial for improving the identification and documentation of euplotid ciliates (Warren et al., 2017). The accumulation of such knowledge can also improve biodiversity estimations and support robust systematics (Schmidt et al., 2007; Foissner et al., 2014; Vďačný and Rajter, 2015; Gao et al., 2016, 2017; Song and Shao, 2017; Sheng et al., 2018; Chen et al., 2019).

The genus *Uronychia* Stein, 1859 is known as a cosmopolitan group, and most species live in a marine habitat (Foissner, 1984; Valbonesi and Luporini, 1990; Song, 1997; Shen et al., 2009; Kim and Min, 2011; Ma et al., 2019). Within the order Euplotida, *Uronychia* is clearly different from other genera as it has a conspicuously hypertrophied undulating membrane that appears horseshoe-like over the oral region, thick and stiffened cirri at the rear end of the body, left marginal cirri and enlarged transverse inserting at concavities of the cell cortex, and enormous sickle-shaped caudal cirri (Song, 1997; Lynn, 2008; Song et al., 2009). However, ultrastructural information about *Uronychia* is still lacking and so far has only been available in *U. transfuga* (Morelli et al., 1996).

In this study, a more complete and detailed ultrastructural study of *U. binucleata* is presented for the first time.

MATERIALS AND METHODS

Sampling, Collection, and Identification

Uronychia binucleata cells were collected from an indoor artificial seawater tank (300 × 80 × 50 cm) in the Laboratory of Protozoology, Ocean University of China, Qingdao, China on September 19, 2018. The seawater tank was constructed in September 2016 by simulating a natural, shallow coastal marine ecosystem during autumn near Jiaozhou Bay (120°20′29′N; 36°03′26′E), Qingdao, China. All components in the tank (i.e., bottom sediment, marine water and marine organisms) were sampled from coastal waters near Jiaozhou Bay and transferred to the seawater tank within two hours. After one month of cultivation, the seawater-tank ecosystem was stable, and the water temperature and salinity were maintained at 25°C and 30‰, respectively. Samples containing bottom sediment and water were collected from the seawater tank. Aliquots were then examined and specimens were isolated using a stereomicroscope. A raw culture was established at room temperature (25°C) and several wheats were added as carbon sources. Specimens used for all subsequent studies were obtain from this raw culture, which was maintained for a year until the study was finished.

Isolated specimens were observed using bright field and differential interference contrast microscopy (Olympus BX 51, Japan). Protargol impregnation was used to reveal the infraciliature and nuclear apparatus according to Wilbert's protocol (Wilbert, 1975). The voucher slide (registration number: ZTY2018091901) with protargol-stained specimens was deposited in the Laboratory of Protozoology (OUC). Identification and general terminology mainly followed Curds and Wu (1983) and Song et al. (2004).

Electron Microscopy

Scanning Electron Microscopy (SEM)

The SEM method was mainly used according to Gu and Ni (1993) and Dong et al. (2020a). The specimens with approximately 1.5 ml of culture medium were transferred into a 1:6 mixture of 1% OsO_4 (diluted from 4% OsO_4 by 30‰ salinity filtering artificial marine water) and saturated solution of $HgCl_2$ for 10 min at room temperature (25°C). Then, the fixed specimens were rinsed with cacodylate buffer and dehydrated in a graded series of ethanol. After that, they were processed sequentially: dried in a critical point dryer (Leica EM CPD300, Leica Microsystems, Wetzlar, Germany), coated with platinum by a sputter coater (Leica EM ACE600, Leica Microsystems, Wetzlar, Germany), and studied with a Hitachi S-4800 (Hitachi, Tokyo, Japan) with an accelerating voltage of 10 kV.

Transmission Electron Microscopy (TEM)

The TEM method mainly followed the procedure of Gu and Ni (1995) and Gu et al. (2002). The first-fix solution contained 200 μl of 2% OsO_4 (diluted from 4% OsO_4 by 30‰ salinity filtering artificial brackish water) and 600 μl of 2.5% glutaraldehyde, and the post-fixed solution contained 2% OsO_4. After being rinsed with cacodylate buffer, the specimens were dehydrated in a graded acetone series and then embedded with Eponate 12 resin. The uranyl acetate and lead citrate were used to stain the ultrathin sections (approximately 70 nm). Finally, a Hitachi HT7700 (Hitachi, Tokyo, Japan) was used to investigate the stained ultrathin sections at an accelerating voltage of 80 kV.

RESULTS

General Morphology of Qingdao Population of *Uronychia binucleata*

The morphology of the population revealed by optical microscopy matched the original description of *Uronychia binucleata* in Song and Wilbert (1997). Thus, only a brief outline is provided to detail the general morphology of the subject we studied: the body size was approximately 75–100 × 60–70 μm, oval to slightly rectangular body shape (**Figures 1A–C**); four frontal, two ventral, and five transverse cirri; three left marginal and three caudal cirri; six dorsal kineties; pattern of buccal apparatus genus-typical (**Figures 1A–H**).

In SEM preparations, an enormous oval buccal field extended over 60% of the ventral region. It was covered by a large undulating membrane (UM, also called paroral membrane) consisting of left and right components. The undulating membrane followed the left and right border of the peristome and were externally sheltered at the base by a prominent cortical

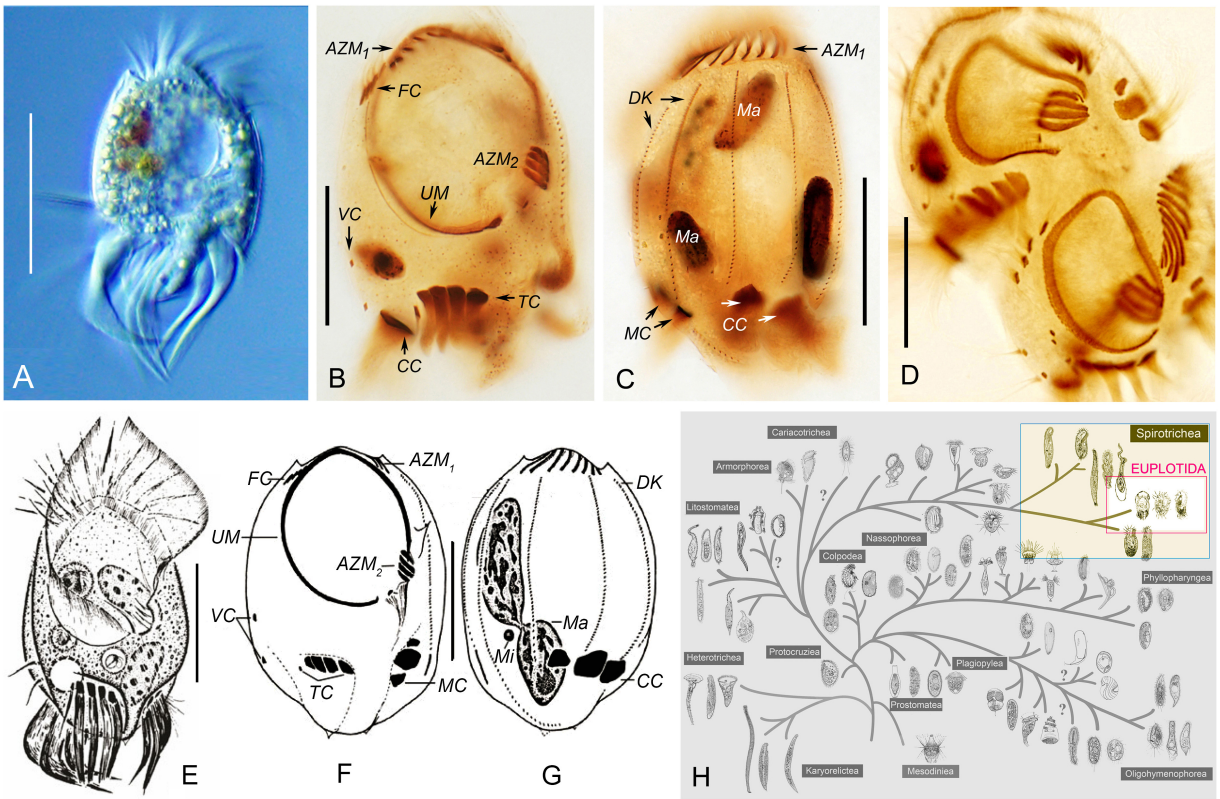

FIGURE 1 | Morphology, infraciliature and taxonomic position of *Uronychia binucleata in vivo* **(A,E)** and after protargol staining **(B–D,F,G)**. **(A,E)** Ventral views of representative individuals. **(B,C,F,G)** Ventral **(B,F)** and dorsal **(C,G)** views, showing nuclear apparatus and infraciliature. **(E–G)** were modified from Song et al. (2009). **(D)** Ventral view of a mid-stage divider. **(H)** Taxonomic positions of *Uronychia binucleata* and related taxa in the hypothetical evolutionary tree of ciliated protozoa according to Gao et al. (2016). Euplotida is highlighted. $AZM_{1,2}$, adoral zone of membranelles 1, 2; CC, caudal cirri; DK, dorsal kineties; FC, frontal cirri; Ma, macronucleus; MC, marginal cirri; TC, transverse cirri; UM, undulating membrane; VC, ventral cirri. Scale bars = 50 μm.

flap (**Figures 2A,C,D,I**). The two components of the undulating membrane were able to close the peristomial cavity, and the right component was always partially covered by the left component in the front (**Figure 2A**). A column of basal bodies that were barren of cilia were arranged along the right side of the right component of the undulating membrane (loss of cilia during preparation cannot be excluded) and could only be observed when the cortical flap was broken (**Figure 2I**). There were two deep concavities on the ventral posterior portion of the body occupied by transverse and left marginal cirri, respectively (**Figures 2A,C,D**). One or two basal body row(s) of transverse and left marginal cirri sometimes lacked cilia (**Figures 2K,L**). Six dorsal kineties were densely inserted in the conspicuous cortical furrows, whose left side was a lifting of the cortex: dorsal kineties 1 and 2 were dorsolaterally located, dorsal kinety 3 was bipolar, and the other three dorsal kineties extended to a deep concavity where caudal cirri emerged (**Figures 2B–D**).

Both ends of the cells were sculpted into spines: (1) Four spines protruded from the anterior end and pointed forward. The rightmost (first) and leftmost (fourth) spine delimited the portion of the anterior part of the adoral zone (AZM_1); the first spine was located on the front left of dorsal kinety 1 and near the margin of the cell; the second and third spines were present in the front of dorsal kineties 2 and 3, respectively, the fourth spine, which was the longest one at approximately 4 μm long, was located between dorsal kineties 3 and 4 (**Figures 2B,C,E,H**). (2) A large spine (approximately 7 μm long) was obvious and situated near the left side of dorsal kinety 1, with the tip oriented toward the cell anterior (**Figures 2C,H**). (3) Two spines usually protruded from the posterior end and pointed backward. One was located under the caudal cirri and on the right side of dorsal kinety 3, and the other was situated under the left marginal cirri and could be observed from the ventral view (**Figures 2B,C,F**).

Ultrastructure of *Uronychia binucleata*

Pellicle

The pellicle was comprised of the typical plasmalemma, which covered the whole cell surface and was subtended by cortical alveoli (**Figures 3B,F,I**). The alveoli were easily distinguished and very electron-lucent; their outer membranes were usually associated with plasmalemma (**Figures 3F,I**). Microtubules were present beneath the inner alveolar membrane and were oriented longitudinally. They were arranged as a single layer in the ventral side and as two layers (showed as triads in a cross section) in the dorsum (**Figures 3B,C**). Densely arranged

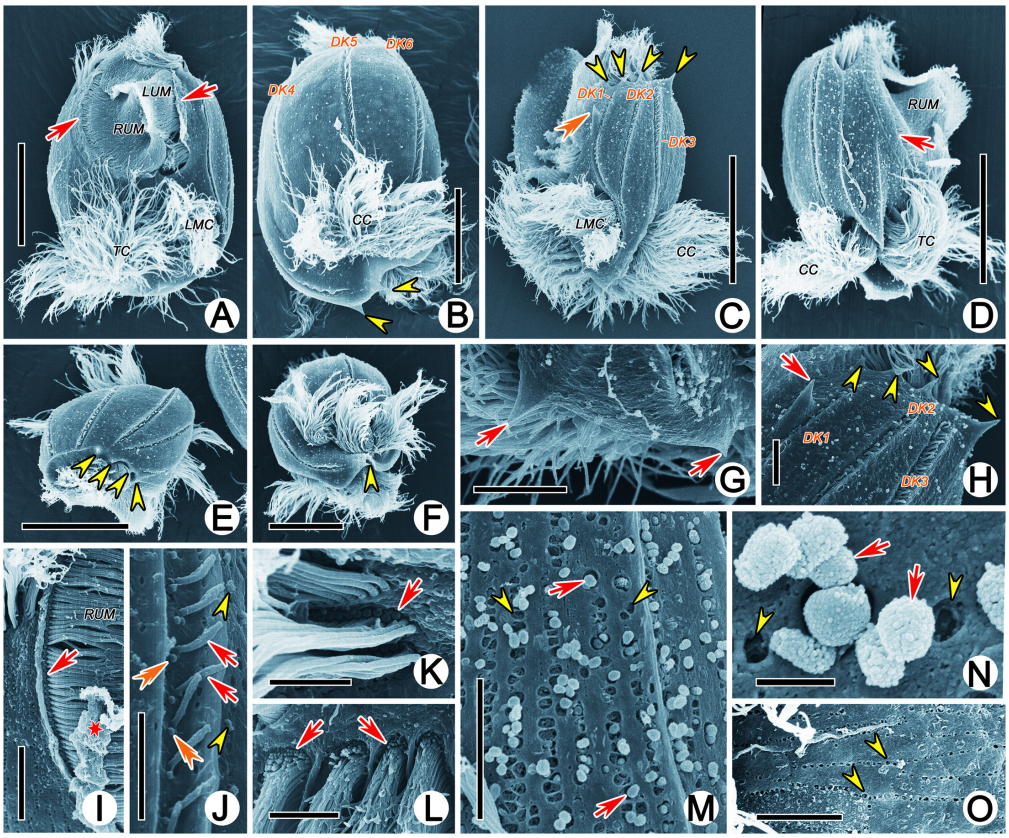

FIGURE 2 | Scanning electron micrographs of *Uronychia binucleata*. **(A–F)** Ventral **(A)**, dorsal **(B)**, left lateral **(C)**, right lateral **(D)**, top **(E)** and bottom **(F)** views of representative individuals. Arrows indicate the cortical flap upon right and left components of the undulating membrane, arrowheads point to the protruding spines of both ends of the cell, double-arrowhead shows the large spine near the left dorsal kinety 1. **(G)** Posterior end of cell to show the two spines (arrows) pointed backward. **(H)** Anterior end of cell showing the four spines (arrowheads) protruding from anterior end and the large spine (arrow) near the left of dorsal kinety 1. **(I)** Proximal of right component of the undulating membrane to show the basal bodies without cilia (arrow). Asterisk indicates the broken cortical flap. **(J)** Cortical groove with dorsal kineties (arrows), showing the two basal bodies, one of which was barren of cilia (double-arrowhead). Arrowheads mark extrusomes. **(K,L)** Basal bodies are barren of cilia (arrows) in left marginal **(K)** and transverse **(L)** cirri. **(M)** Extruding or extruded extrusomes (arrows) arranged in short rows. Arrowheads point to residual "pits." **(N)** Apical view of extruded extrusomes (arrows) sticking together. Arrowheads show residual "pits." **(O)** Residual "pit" (arrowhead) after extrusome has been extruded, arranged in short rows. CC, caudal cirri; DK1–6, dorsal kineties 1–6; LMC, left marginal cirri; LUM, left component of the undulating membrane; TC, transverse cirri; RUM, right component of the undulating membrane. Scale bars = 30 μm **(A,C–E)**, 20 μm **(B,F)**, 5 μm **(G–I,L,M,O)**, 3 μm **(J)**, 2 μm **(K)**, 0.5 μm **(N)**.

vesicular structures were located beneath the subpellicular microtubules and were usually accompanied by extrusomes, especially in the dorsal cortex (**Figures 3A,E–G,I**). They were bounded by unit membranes and had low electron density. Vesicular structures and extrusomes were always restricted by numerous microtubules, thus appearing as rectangle-like instead of spherical (**Figures 3D–H**). In some longitudinal sections of cortical lifting near the dorsal kineties, the subpellicular microtubule layer and extrusomes occurred as two closely associated distinct layers (i.e., microtubules and extrusomes distributed at intervals beneath the inner alveolar membrane; **Figure 3D**). No perilemma or epiplasm were observed.

Cortical Granules (Extrusomes)

Cortical granules were not observed *in vivo*; however, numerous spherical or ovoidal, rough-surfaced, extruded granules (approximately 0.5 μm in diameter) were present on the dorsal and ventral surfaces and even in the cortical grooves occupied by dorsal kineties in SEM preparations (**Figures 2A–D,J**). They were arranged longitudinally in short (including 10 granules at most) or long rows (including more than 50 granules) (**Figures 2M,N**). Residual "pits" could be observed (**Figure 2O**). In TEM preparations, the cortical granules were mostly located in the cortex in long or short longitudinal rows that were distinguishable with SEM (**Figure 3A**), while they were densely clustered in the buccal field (**Figure 4B**) and near cirri (**Figure 4C**). They appeared as ovoidal or even rectangle-like because of the restriction of microtubules, and each was bounded by a unit membrane with content of varying electron density (**Figures 3D–H, 4A–D**). Some granules with lower electron density content were more diffuse, possibly reflecting various stages of extrusion (**Figures 4D–H**).

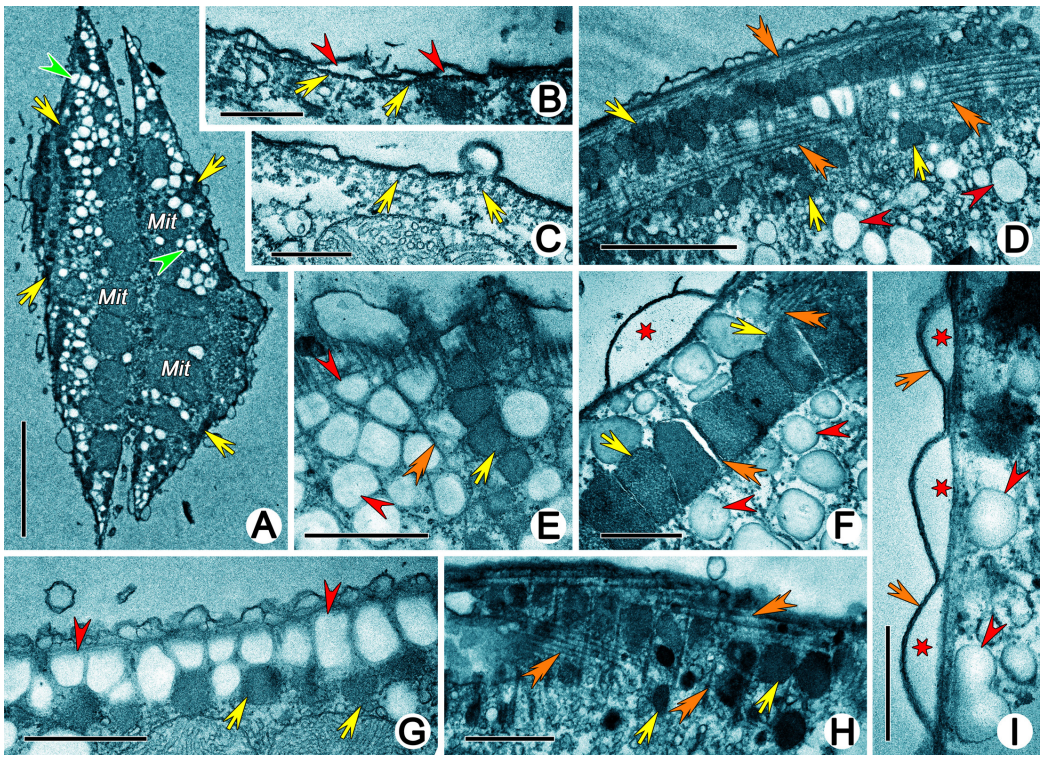

FIGURE 3 | Transmission electron micrographs of cortex of *Uronychia binucleata*. **(A)** Longitudinal section of cell near dorsal surface, showing the arrangement of extrusomes (arrows), vesicular structures (arrowheads) and mitochondria (Mit). **(B,C)** Subpellicular microtubules (arrows) arrange singularly in venter **(B)** and as triads in dorsum **(C)**. Arrowheads mark alveoli. **(D)** Subpellicular microtubules (double-arrowheads) and extrusomes (arrows) distribute at intervals, which might be the longitudinal section of cortical grooves occupied by dorsal kineties. Arrowheads point to vesicular structures. **(E–G)** Vesicular structures (arrowheads) and extrusomes (arrows) are restricted by numerous microtubules (double-arrowheads) and showed as rectangle-like. Asterisk indicates alveolus. **(H)** Extrusomes (arrows) distribute among microtubules (double-arrowheads). **(I)** Cortex region, showing plasmalemma (arrows), alveoli (asterisks) and vesicular structures (arrowheads). Mit, mitochondria. Scale bars = 5 μm **(A)**, 0.5 μm **(B,C,F,I)**, 2 μm **(D)**, 1 μm **(E,G,H)**.

Somatic Ciliature

The fine structure of some fibrillar structures of ciliature (i.e., dikinetids and polykinetids) were revealed as follows by TEM. (1) The dorsal bristle units were in a dikinetid pattern: two kinetosomes were linked by an electron-dense inter-kinetosomal connective; a tangential transverse ribbon was located in front of the anterior kinetosome; and a kinetodesmal connection was associated with posterior kinetosome (**Figure 5B**). (2) The caudal cirri and transverse cirri were polykinetids. Their connective fibers were similar: the kinetosomes were linked to each other in the same row by electron-dense double linkages containing anterior and posterior connections (AC and PC) and were attached to the anterior and posterior kinetosomes in the next row at triplet position by diagonal connections (DC, also called oblique fibrils/connections or diagonal fibrils) and transverse connections (TC, also called transverse fibril or zig-zag fibril) (**Figures 5E,K**, **8A**).

Structures in Buccal Field

The adoral zone of membranelles (AZM) were bipartite and distributed in two distinct zones (i.e., the anterior (AZM_1) and posterior (AZM_2) parts of the adoral zone membranelles; **Figure 1B**). Each membranelle in AZM_2 consisted of three rows of kinetosomes (**Figure 5G**). The diagonal connection interconnected the diagonal row and, upon reaching the most posterior row, extended to contact the electron-dense material called the radial ribbon of microtubules (**Figures 5H**, **8B**). The double linkages (containing anterior and posterior connections) that were parallel to the long rows linked two kinetosomes in the same row (**Figures 5H**, **8B**). The terminal fiber emerged from the right side of each row of kinetosomes (**Figures 5H**, **8B**).

The details of the undulating membrane (including right and left components) were revealed as follows: (1) The undulating membrane contained more than five rows of kinetosomes (**Figures 5F–J**). In a cross section, the connections between kinetosomes of undulating membrane were similar to other cirri, which showed as a polykinetid pattern: the diagonal and longitudinal connection (LC, also called longitudinal fibril) linked the two diagonal kinetosomes in different rows, and double linkages (containing anterior and posterior connections) that were parallel to the long rows connected kinetosomes in the same row (**Figures 5F–J**, **8C**). The interconnecting diagonal connection formed a series of crescent-like structures at the longitudinal innermost part (**Figure 5D**). (2) A series of continuous fibrous layers with condensation knobs beneath the kinetosomes connected the kinetosomes in the right and left

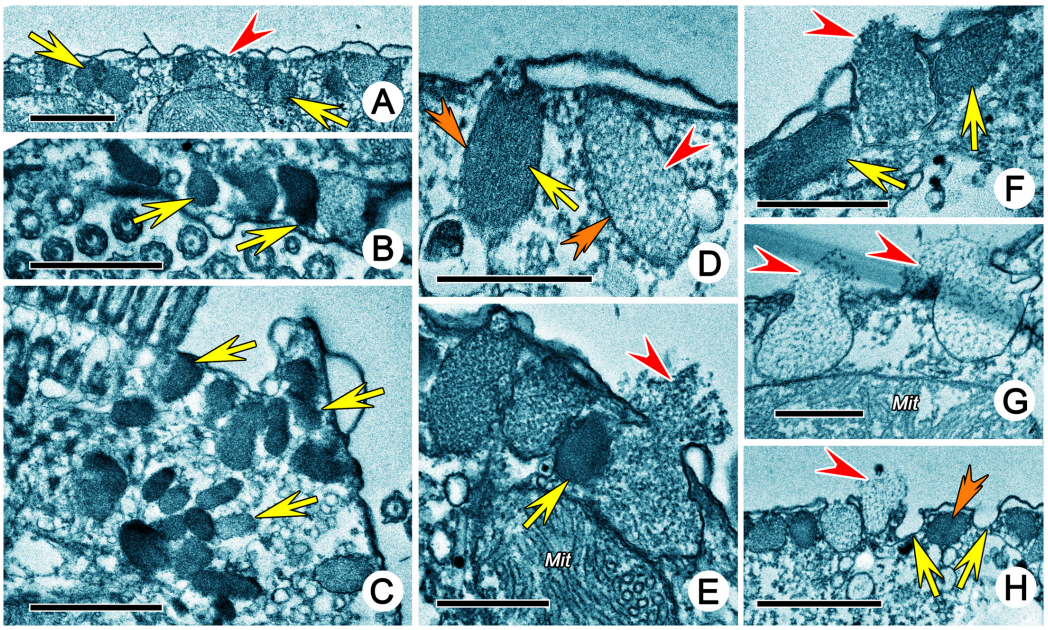

FIGURE 4 | Extrusomes of *Uronychia binucleata* in the transmission electron micrographs. **(A)** Extrusomes (arrows) under pellicle. Arrowhead marks microtubule. **(B,C)** Sections near the buccal region **(B)** and cirri **(C)**, showing the arrangement of extrusomes (arrows) in buccal region **(B)** and around cirri **(C)**. **(D)** Extrusomes with different electron density, arrow points to the electron-dense extrusome, while arrowhead points to the electron-lucent extrusome. Double-arrowheads indicate the unit membrane around extrusomes. **(E–G)** Longitudinal section of extrusomes, showing the fusion of extrusome membrane with pellicle and extruding of diffuse content (arrowheads). Arrows point to extrusomes which are not extruding. **(H)** Section perpendicular to pellicle showing extrusomes with different stages of extrusion: resting (double-arrowhead), extruding (arrowhead) and extruded (arrows show the membrane of extrusome which remains in place after extrusion). Mit, mitochondria. Scale bars = 1 μm **(A–C,H)**, 0.5 μm **(D–G)**.

components of the undulating membrane at the anterior part (**Figure 5C**). (3) Four membrane structures contained cytoplasm, small vesicles, microtubules and extrusomes arranged in a single layer bounded by unit plasmalemma (**Figures 5A**, **6C–G**). The membrane structures located outside the right and left components of the undulating membrane originated from plasmalemma, while those located inside the two components of the undulating membrane extended from plasmalemma of the dorsal wall of the buccal cavity (**Figures 5A**, **6C–E**). In some sections, one or two layer(s) of rootless membrane structures were present beneath the left component (**Figures 6A,D,E**). The membrane structures situated outside the undulating membrane might be the cortical flap observed in SEM.

A large complicated cytopharyngeal apparatus was observed in TEM which extended into cytoplasm as a narrow L-shaped cavity and might be opened at the base of the left component of the undulating membrane (**Figures 6A,B**). The cortex composition of the buccal area was similar, with a pellicle, containing plasmalemma, alveoli, and subpellicular microtubules (**Figure 6J**). Numerous electron-lucent flattened pharyngeal disks were present, interposed with microtubular sheets, located in three parts: (1) beneath the dorsal wall of the buccal cavity (**Figures 6A,H**); (2) at the innermost end of the cytopharyngeal apparatus (**Figures 6B,L**); and (3) at the bottom corner and arm of the cytopharyngeal apparatus (**Figures 6A,K**). A microtubules sheet was present beneath the cytopharyngeal apparatus (**Figures 6B,I**).

Cytoplasm, Cytoplasmic Organelles and Nuclear Apparatus

The cytoplasm was an electron-lucent colloidal matrix containing numerous granules, electron-lucent vesicles, cytoplasmic organelles, and various cytoplasmic inclusions such as lithosomes (**Figures 7E,G**). The lithosomes were globule concentric concretions with multiple lamellae (**Figure 7G**). Some irregularly shaped concentric concretions might also be lithosomes (**Figure 7E**). The mitochondria were approximately 3 μm long, ellipsoidal with tubular cristae and mainly distributed beneath the pellicle (**Figures 7A,F**). Food vacuoles were approximately 5 μm in diameter and contained large amounts of food debris, possibly of bacterial origin (**Figure 7H**). Macronuclear nodules were surrounded by a karyotheca and contained irregular chromatin bodies that were more or less homogenous and several spherical nucleoli that contained scattered, punctate, electron-dense particles (**Figures 7B–D**). A replication band (RB), which consisted of two zones of chromatin reorganization (reticular zone, RZ and diffuse zone, DZ), was present in the macronuclear nodules when numerous chromatin bodies with homogenous electron density were embedded in the macronuclear nodules (**Figures 7B,D**). The movement direction of the RB through the nucleus was observed from DZ to RZ, whereby dense chromatin bodies in the front RB were organized as RZ and the reticular chromatin were then organized as DZ, which contributed to the reconstitution of dense chromatin bodies behind the RB (**Figures 7B,D**).

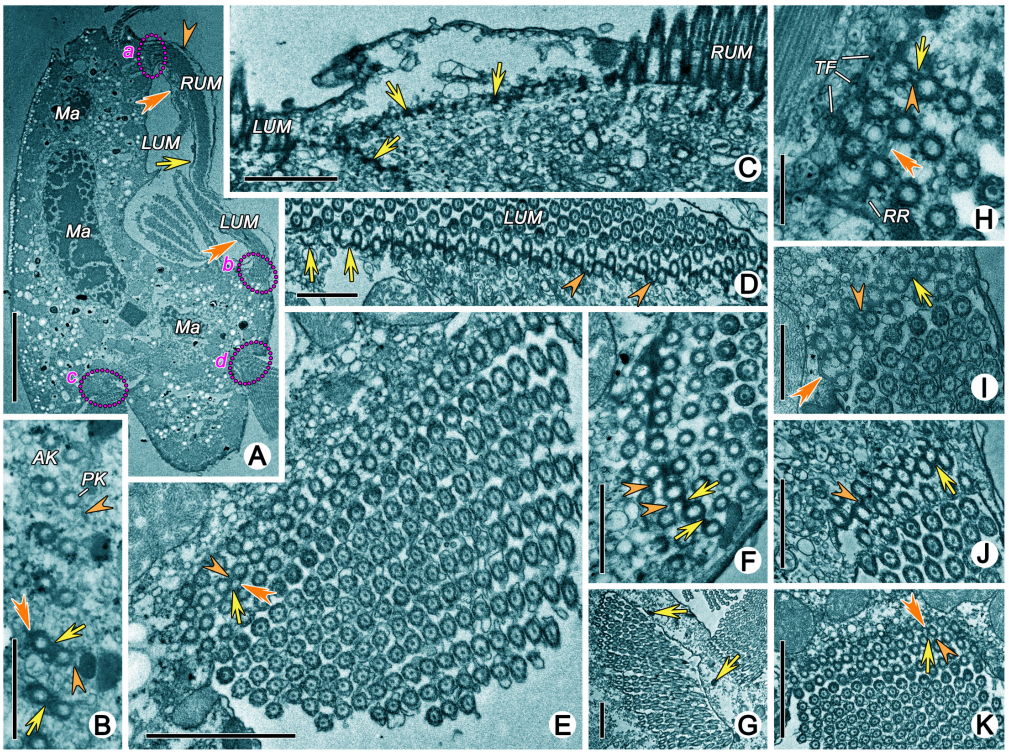

FIGURE 5 | Transmission electron micrographs of ciliature of *Uronychia binucleata*. **(A)** Longitudinal section of cell from right lateral view, to show the membrane structure located outside of right component of the undulating membrane (arrowhead), inside of right component of undulating membrane (arrows), and inside of left component of the undulating membrane (double-arrowhead). Areas marked "a" "b" "c" and "d" are enlarged in **(J,F,E,K)**, respectively. **(B)** Oblique section of dorsal kineties, showing the connections between the anterior (AK) and posterior (PK) kinetosomes. Arrows mark the inter-kinetosomal connective, arrowheads point to kinetodeamal fiber, double-arrowhead indicates the tangential transverse ribbon. **(C)** Section of anterior part of cell showing continuous fibrous layer (arrows) connects the kinetosomes in left and right components of the undulating membrane. **(D)** Cross section of left component of the undulating membrane, to show the show the diagonal connections (arrowheads), some of which forms a series of crescent-like structures (arrows). **(E)** Cross section of caudal cirri, showing the connections among kinetosomes. Arrowhead marks the double linkages between kinetosomes in the same row, arrow points to the diagonal connection, and double-arrowhead indicates the transverse connection. **(F,I,J)** Cross section of left **(F,J)** and right **(I)** components of the undulating membrane showing the kinetosomes linked by double linkages (arrows) and diagonal connections (arrowheads). Double-arrowhead marks a crescent-like structure in left component of the undulating membrane. **(G)** Cross section of adoral zone of membranelles 2 consisting of three rows in each membrane. Arrows point to the extrusomes. **(H)** Detailed magnification of a membrane from adoral zone of membranelles 2, to show the diagonal connection (double-arrowhead) interconnects posterior row and extends out to form radial ribbon of microtubules (RR). Arrow points to anterior connection, arrowhead marks the posterior connections. **(K)** Cross section of transverse cirri. Arrowhead marks electron-dense double linkages linked kinetosomes in the same row, arrow points to the diagonal connection, double-arrowhead indicates the transverse connection. AK, anterior kinetosome; LUM, left component of the undulating membrane; Ma, Macronuclear nodule; PL, posterior kinetosomes; RUM, right component of the undulating membrane; RR, radial ribbon of microtubules; TF, terminal fiber. Scale bars = 10 μm **(A)**, 1 μm **(B–D,F,I,J)**, 2 μm **(E,G,K)**.

The micronuclei contained numerous chromatin bodies of homogenous electron density (**Figure 7C**).

Conclusion

A summary of the present research regarding *Uronychia binucleata* is as follows.

(i) Visual general morphology was observed by SEM, including obvious spines and left and right components of the undulating membrane.

(ii) Details concerning the complicated cortex were elaborated upon. In short: numerous electron-lucent vesicular structures that are usually accompanied by cortical granules (extrusomes) always showed as rectangle-like because of the restriction of microtubules. The cortical granules were not observed *in vivo*; however, they showed as 0.5 μm in diameter, spherical or ovoidal in shape, rough-surfaced, arranged in longitudinal rows in SEM, with varying electron density in TEM.

(iii) The undulating membrane was highly developed, including right and left components, flanked by a prominent cortical flap. Four membrane structures were situated inside and outside of the right and left components of the undulating membrane, respectively.

DISCUSSION

Ultrastructural Features of Pellicle

The organization of a typical ciliate pellicle is generally composed of a continuous plasmalemma, alveoli that are subtended by a

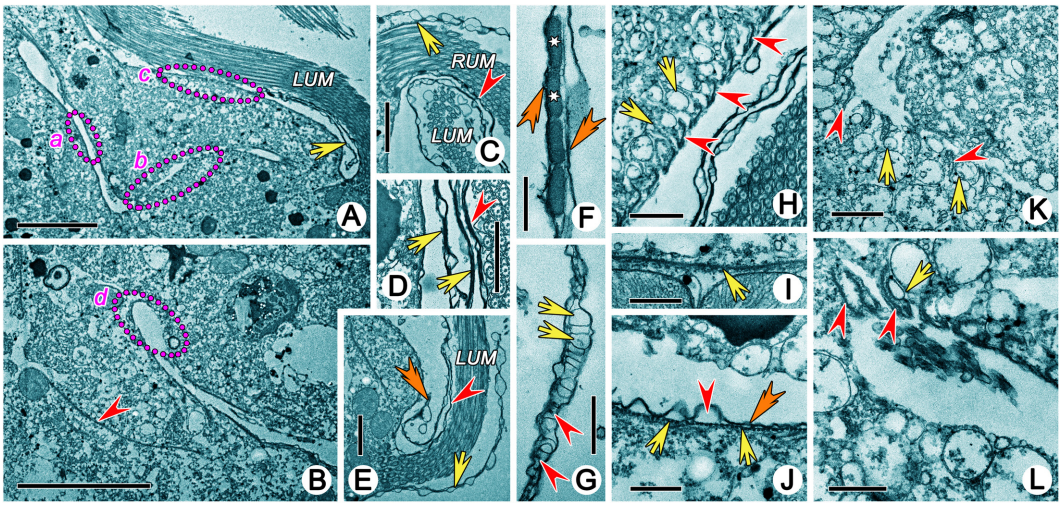

FIGURE 6 | Transmission electron micrographs showing structures in buccal field of *Uronychia binucleata*. **(A,B)** Longitudinal section of buccal field, showing the large cytopharyngeal apparatus which extended into cytoplasm as a narrow L-shaped cavity. Areas marked "a" "b" "c" and "d" are enlarged in **(J,K,H,L)**, respectively. Arrow marks the rootless membrane structure beneath the left component of the undulating membrane, arrowhead points to the microtubules sheet beneath the cytopharyngeal apparatus. **(C,E)** Base of right **(C)** and left **(E)** components of the undulating membrane, to show the membrane structures around it extending from plasmalemma of dorsal wall (arrowhead) and cell surface (arrow). Double-arrowhead points to the rootless membrane structure. **(D)** Longitudinal section of membrane structures. Arrowhead indicates membrane structure inside of left component of the undulating membrane, arrows point the rootless membrane structures. **(F,G)** The membrane structure contains numerous small cytoplasmic vesicles (arrows), microtubules (arrowheads) and extrusomes (asterisk) and is bounded by the plasmalemma (double-arrowheads). Flattened pharyngeal disks (arrows) situated in the dorsal wall of the buccal cavity **(H)**, at the innermost end **(K)** and bottom corner of cytopharyngeal apparatus **(L)**. Arrowheads point to the microtubular sheets interposed between them. **(I)** Microtubules sheet (arrow) located beneath the cytopharyngeal apparatus. **(J)** Cytopharyngeal apparatus contains plasmalemma (double-arrowhead), alveoli (arrowhead) and subpellicular microtubules (arrow) without pharyngeal disks. LUM, left component of the undulating membrane; RUM, right component of the undulating membrane. Scale bars = 5 μm **(A,B)**, 2 μm **(C,E)**, 1 μm **(D,H,K)**, 0.5 μm **(F,G,I,L)**.

membrane, and underlying fibrous epiplasm (Pitelka, 1965; Lynn, 2008). In euplotids, such as in *Aspidisca* (Rosati et al., 1987), *Certesia* (Wicklow, 1983), *Euplotes* (Ruffolo, 1976; Foissner, 1978; Hausmann and Kaiser, 1979) and *Euplotidium* (Lenzi and Rosati, 1993), the alveolar plates were filled with electron-dense material, mainly composed of protein, thus also called platein (Kloetzel, 1991). The alveolar plates appeared to lend form and rigidity to the cell cortex, replacing the epiplasm of other ciliates (Kloetzel, 1991). However, neither the alveolar plates nor the epiplasm could be observed in *Uronychia transfuga* by Morelli et al. (1996), which was the only ultrastructural research on the genus *Uronychia* before our present work. The same result occurred in *U. binucleata* in our research.

The subpellicular microtubules, which are essential parts of the cortex, extend longitudinally beneath the pellicle (Lynn, 2008). Grim (1967) gives a detailed description of the organization and orientation of subpellicular microtubules in *Euplotes*: a series of closely associated longitudinal tubules form a triad configuration (called microtubular triads) in the dorsal, while appearing in a single configuration in the ventral (Ruffolo, 1976; Foissner, 1978; Grim et al., 1980; Fukang and Lingmei, 1996; Schwarz et al., 2007). In this research, the similar arrangement of subpellicular microtubules described by Grim (1967) was also present in *U. binucleata*. However, only a sheet of subpellicular microtubules was described in *U. transfuga* (Morelli et al., 1996), which could mean that the triad configuration in the dorsal was ignored. These kinds of subpellicular microtubules were rarely reported until now, which have only been observed in some euplotids (Rosati, 1970; Wicklow, 1983; Rosati et al., 1987; Gong et al., 2018) and some cyrtophorids (Hofmann and Bardele, 1987; Kurth and Bardele, 2001), thus, we speculate that the arrangement of the subpellicular microtubules might be one of characteristics of the order Euplotida. The function of these kind of arrangements of subpellicular microtubules is still ambiguous, they may be used for support or remarkable rigidity (Sandborn et al., 1964; Gliddon, 1966), sensory conduction or coordination (Randall and Jackson, 1958; Jerka-Dziadosz et al., 1987; Arregui et al., 1994), and fluid conduction (Sandborn et al., 1964).

In addition, numerous electron-lucent sac-like vesicular structures, arranged densely below the subpellicular microtubules could be seen clearly in TEM. These structures have never been reported in other euplotids or hypotrichs until now, and their function is still ambiguous. Thus, further investigations on these vesicular structures are needed in order to fully characterize them and determine their function.

Cortical Granules of *Uronychia binucleata* Are Not Ampules

The cortical granules of *Uronychia binucleata* are membrane-bound organelles that can be extruded and expel their contents to the outside of the cell, which conforms with the definition of extrusomes given by Hausmann (1978).

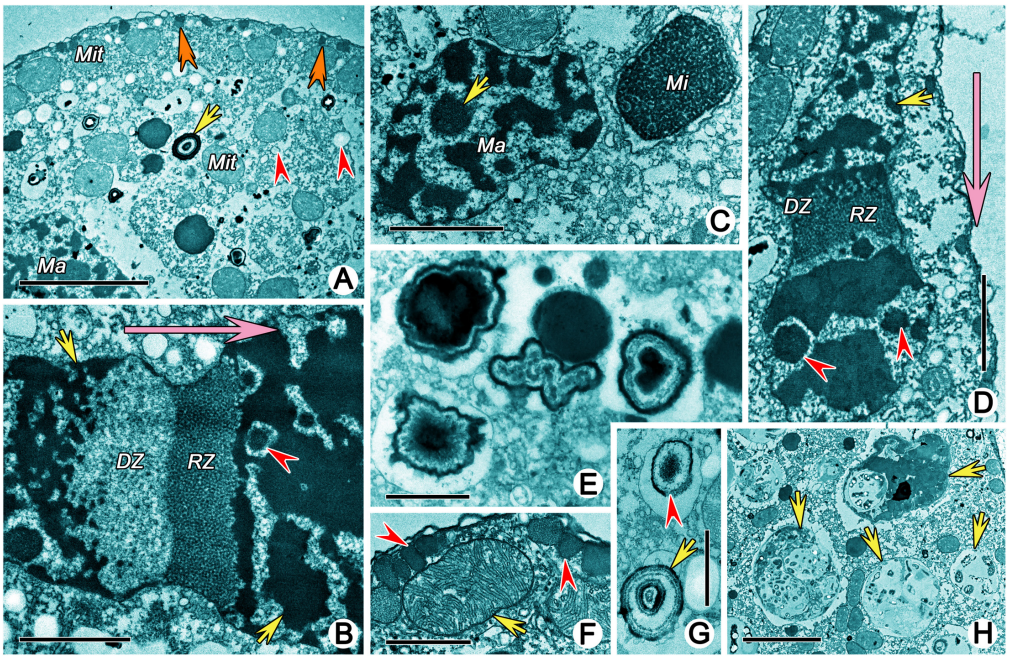

FIGURE 7 | Transmission electron micrographs showing structures in cytoplasm of *Uronychia binucleata*. **(A)** Cytoplasm and cytoplasmic organelles. Arrow marks the lithosome, arrowheads point to vesicles, double-arrowheads indicate the extrusomes. **(B,D)** Replication band is composed of a reticular zone (RZ) and a diffuse zone (DZ). Arrowheads point to nucleoli, arrows mark chromatin bodies, big arrows indicate the movement direction of the replication band. **(C)** Macronuclear nodule and micronucleus. Arrow marks the nucleolus. **(E)**Various shaped concentric concretions which might be lithosomes. **(F)** Section perpendicular to pellicle showing the micronucleus (arrow) and extrusomes (arrowheads). **(G)** Lithosome (arrow) and concentric concretions (arrowhead). **(H)** Food vacuoles containing bacteria. Ma, Macronuclear nodule; Mi, micronucleus; Mit, mitochondria. Scale bars = 5 μm **(A,H)**, 2 μm **(B–D)**, 1 μm **(E,F)**, 0.5 μm **(G)**.

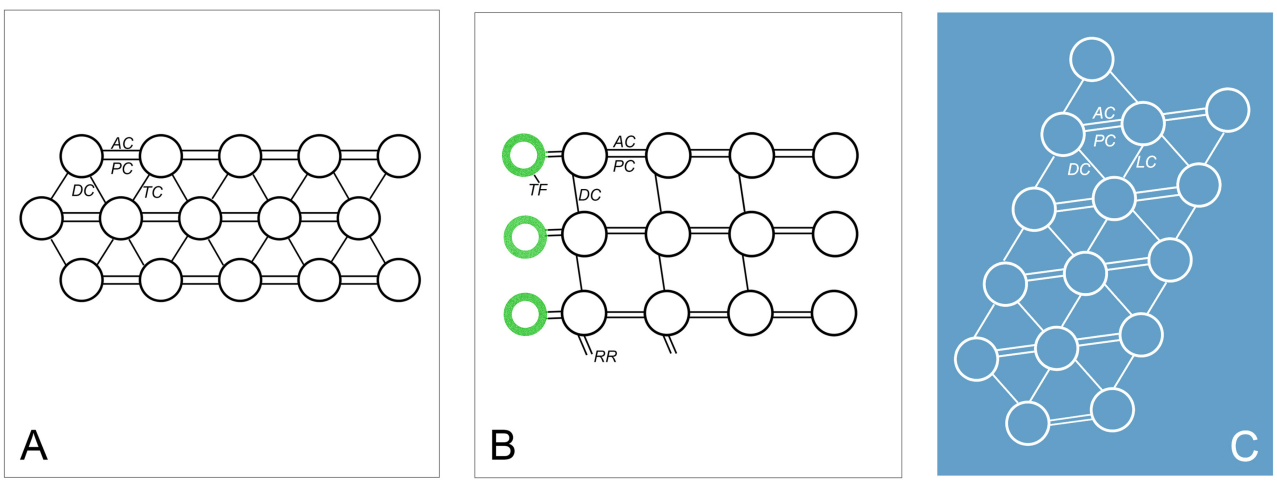

FIGURE 8 | Diagrammatic drawings of the connections of oral and somatic ciliature in *Uronychia binucleata*. **(A)** Scheme of caudal cirri and transverse cirri showing the anterior (AC) and posterior connections (PC) link kinetosomes in the same row, diagonals (DC) and transverse connections (TC) link kinetosomes in the next row. **(B,C)** Scheme representation of cross section of posterior part of adoral zone membranelles **(B)** and undulating membrane **(C)**. AC, anterior connection; DC, diagonals connection; LC, longitudinal connection; PC, posterior connection; RR, radial ribbon of microtubules; TF, terminal fiber.

As a special type of mucocyst, the ampules are defined by Ruffolo (1976) as membrane-bound organelles in association with both dorsal bristles and compound ciliary organelles of the ventral surface (i.e., arranged around the dorsal bristles or ciliary insertion as a "rosette" or "spokes" (Fauré-Fremiet and André, 1968; Ruffolo, 1976). Moreover, this is often considered one of the characteristics of euplotids (Lynn, 2008), as reported in *Euplotes* (Verni et al., 1978; Dallai and Luporini, 1981; Görtz, 1982; Rosati and Modeo, 2003; Lobban et al., 2005), *Diophrys* (Rosati, 1970; Gong et al., 2018), *Certesia* (called muciferous-like bodies;

Wicklow, 1983) and *Aspidisca* (called cytoplasmic vesicles; Rosati et al., 1987). However, the characteristic extrusomes of *Uronychia* can be easily differentiated from these ampules as follows: (1) they are not observed *in vivo* vs. being distinctive *in vivo*; (2) they are arranged in longitudinally oriented rows vs. around the dorsal bristles or ciliary insertion as a "rosette"; (3) most notably, they can be extruded vs. no extrusion process being observed (Fauré-Fremiet and André, 1968; Rosati, 1970; Ruffolo, 1976; Görtz, 1982; Wicklow, 1983; Rosati et al., 1987; Gong et al., 2018). That is to say, in *Uronychia*, as a notable member of Euplotida, the ampules may not exist. However, this is still waiting to be confirmed by further research on other species of *Uronychia*.

Fibrillar Structures of Cirri

As the basis of ciliature, research on the component structures of the ciliate kinetids has a long history. Lynn (1976) defined the monokinetids, dikinetids and polykinetids as kinetids composed of one, two and more than two kinetosomes, respectively, to avoid the confusion implicit in ciliary apparatus, such as a cirrus, a membranelle, or any complex assemblage. Three patterns of polykinetids were classified by Lynn (1981): (1) *Phacodinium* pattern: eight or nine kinetosomes arranged as longitudinal rows and linked by two tangentially oriented transverse ribbons (Didier and Dragescjo, 1979); (2) *Plagiotoma* pattern: two and nine kinetosomes linked by dense material (Albaret and Grain, 1973); and (3) hypotrich pattern: a number of kinetosomes arranged hexagonally and linked in a complex manner, for example, in *Gastrostyla steinii*, *Oxytricha fallax*, *Stylonychia mytilus* and *Euplotes eurystomus* (Gliddon, 1966; Grim, 1972; Grimes, 1972; de Puytorac et al., 1976). The first two types mainly exist in groups of lower forms of ciliates, while the third type is present in hypotrichous and euplotid ciliates. However, in Euplotida two types of kinetosome connections have been reported to date: (1) a single longitudinal connection linking the two kinetosomes in different rows is observed in Uronychiidae and Aspidiscidae, represented by *U. binucleata* (the count of longitudinal connection in *U. transfuga* is not mentioned) and *Aspidisca* sp., respectively (Rosati et al., 1987; Morelli et al., 1996); (2) a double longitudinal connection between kinetosomes in different rows, which is present in the species of Euplotidae (represented by *E. eurystomus*) and Certesiidae (represented by *Certesia quadrinucleata*) (Gliddon, 1966; Wicklow, 1983). *U. binucleata* belongs to the hypotrich pattern with a single longitudinal connection. It is worth mentioning that in the subclass Hypotrichia, the single longitudinal connection is present in Urostylida (e.g., *Paraurostyla weissei*, *Pseudokeronopsis carnea,* and *Pseudourostyla cristata*) while the double longitudinal connection is observed in Sporadotrichida (e.g., *Gastrostyla steinii, Oxytricha fallax,* and *Stylonychia mytilus*) (Gliddon, 1966; Grimes, 1972; de Puytorac et al., 1976; Grimes and L'hernault, 1978; Wirnsberger and Hausmann, 1988; Jerka-Dziadosz and Wiernicka, 1992; Sun et al., 2018). Unfortunately, the data about component structures of the ciliate kinetids is too limited. Furthermore, a TEM-based integrative approach is needed in order to improve the characterization of the structures for research systematics. In conclusion, the variations of component structures of ciliate kinetids revealed that some degree of evolutionary divergence might have occurred in the modifications of a common structural theme. How this divergence is assigned to different higher-level taxonomic groupings remains a challenge in ciliate systematics (Rosati et al., 1987).

Ultrastructural Features in Buccal Field

The conspicuousness and the peculiar organization of the oral membrane distinguishes the *Uronychia* from the members of the Euplotida (Foissner, 1984; Valbonesi and Luporini, 1990; Song, 1997; Shen et al., 2009; Kim and Min, 2011; Ma et al., 2019). As an important characteristic of the genus *Uronychia*, this structure has been described in most species at the light optical level (Borror, 1979; Wilbert and Kahan, 1981; Hill, 1990; Song and Wilbert, 1997; Shen et al., 2009; Kim and Min, 2011; Shi et al., 2017; Ma et al., 2019) and some with SEM (Hill, 1990; Valbonesi and Luporini, 1990; Leonildi et al., 1998), though not in detail. Morelli et al. (1996) provided the ultrastructure based on *U. transfuga*, detailing the organization of cilia and its feeding behavior, called upstream filtration. However, the special membrane structure around the undulating membrane was not mentioned. In the present study, four membrane structures are inside and outside the right and left components of the undulating membrane, respectively, which suggests that the undulating membrane is bounded by a cortical flap. It is worth noting that one or two layer(s) of rootless membrane structures are sometimes present beneath the right component of the undulating membrane, which might be caused by two circumstances: (1) the cortical flap curves and cuts twice; or (2) it is the buccal seal (Foissner and Al-Rasheid, 2006; Berger, 2008; Dong et al., 2020a).

The pharyngeal disks in the oral region are the precursors that rapidly form food vacuole membranes (Kloetzel, 1974; Lynn, 2008). They have been classified into two types by Dong et al. (2020b): (1) Single-membrane-bound pharyngeal disks with low electron density (for example, in *Climacostomum virens*, *Euplotidium itoi*, *Parabistichella variabilis* and *Uronychia transfuga*) and (2) myeloid pharyngeal disks with high electron density (for example, in *Euplotes eurystomus*, *Certesia quadrinucleata*, *Diophrys oligothrix* and *D. scutum*) (Fauré-Fremiet and André, 1968; Kloetzel, 1974; Fischer-Defoy and Hausmann, 1981; Wicklow, 1983; Rosati et al., 1987; Lenzi and Rosati, 1993; Morelli et al., 1996; Verni and Gualtieri, 1997; Gong et al., 2018). The single-membrane-bound pharyngeal disks are present in *U. binucleata*, interposed with microtubular sheets as reported in *U. transfuga* (Morelli et al., 1996). Thus, it could be the typical module of pharyngeal disks in *Uronychia*. It is noteworthy that the pharyngeal disks of *U. binucleata* are divided into three parts, which has not been noted either in *U. transfuga* or other ciliates (Morelli et al., 1996).

CONCLUSION

The major findings of our study can be summarized as follows:

(i) The pellicle of *U. binucleata* not only has typical euplotid features, such as plasmalemma, alveoli and highly

organized subpellicular microtubules, but in addition has unique distinctive characteristics. These are a lack of alveolar plates and of an epiplasm, as well as abundant electron-lucent sac-like vesicular structures arranged densely below the subpellicular microtubules.

(ii) The cortical granules (extrusomes) of *U. binucleata* are mucocyst-like instead of the typical ampules.

(iii) The component structures of the ciliate kinetids of *U. binucleata* belong to the hypotrich pattern with a single longitudinal connection.

(iv) The special membrane structures are inside and outside the right and left components of the undulating membrane, respectively, suggests that the undulating membrane is bound by a cortical flap.

(v) The pharyngeal disks of *U. binucleata* are of a single-membrane-bound type.

These features clearly distinguish the Uronychita from other members of the Euplotida, and will improve the diagnosis of this evolutionary lineage. This finding is relevant not only for advancing systematics, but also for reconstructing the evolutionary history of ciliated protists, and for assessing community composition in ecological studies.

DATA AVAILABILITY STATEMENT

The original contributions presented in the study are included in the article/supplementary material, further inquiries can be directed to the corresponding author/s.

AUTHOR CONTRIBUTIONS

HM and XF conceptualized the project. JD carried out the research. TZ carried out the identification by live observation and protargol staining. JD, LL, XF, TZ, and TS helped data interpretation, wrote and revised the manuscript. All authors approved the final version of the manuscript.

FUNDING

This work was supported by the Marine S&T Fund of Shandong Province for Pilot National Laboratory for Marine Science and Technology (Qingdao) (2018SDKJ0406-1), the National Nature Science Foundation of China (Project Nos: 31772431 to LL; 41876151 to XF; 32070432 to HM and M. Miao), and Researchers Supporting Project Number (RSP-2020/7) of King Saud University, Riyadh, Saudi Arabia.

ACKNOWLEDGMENTS

We thank Prof. Weibo Song (Ocean University of China, China) for his generous help and advice on preparing the manuscript and Dr. Bing Ni (East China Normal University, China) for his helpful guidance in SEM and TEM.

REFERENCES

Albaret, J., and Grain, J. (1973). L'ultrastructure de *Plagiotoma lumbrici* Dujardin (Cilié Hétérotriche). *Protistologica* 9, 221–234.

Arregui, L., Serrano, S., and Guinea, A. (1994). Microtubular elements of the marine antarctic ciliate *Euplotes focardii* (Ciliophora, Hypotrichia). *Arch. Protistenk.* 144, 357–364. doi: 10.1016/S0003-9365(11)80238-1

Berger, H. (2008). Monograph of the amphisiellidae and trachelostylidae (Ciliophora, Hypotricha). *Monogr. Biol.* 88, 1–737. doi: 10.1007/978-1-4020-8917-6_1

Borror, A. C. (1979). Redefinition of the urostylidae (Ciliophora, Hypotrichida) on the basis of morphogenetic characters. *J. Protozool.* 26, 544–550. doi: 10.1111/j.1550-7408.1979.tb04192.x

Chen, X., Jiang, Y., Gao, F., Zheng, W., Krock, T. J., Stover, N. A., et al. (2019). Genome analyses of the new model protist *Euplotes vannus* focusing on genome rearrangement and resistance to environmental stressors. *Mol. Ecol. Resour.* 19, 1292–1308. doi: 10.1111/1755-0998.13023

Chen, X., Wang, Y., Sheng, Y., Warren, A., and Gao, S. (2018). GPS it: an automated method for evolutionary analysis of nonculturable ciliated microeukaryotes. *Mol. Ecol. Resour.* 18, 700–713. doi: 10.1111/1755-0998.12750

Curds, C. R., and Wu, I. C. H. (1983). A review of the Euplotidae (Hypotrichida, Ciliophora). *Bull. Br. Mus. Nat. Hist. (Zool.)* 44, 191–247.

Dallai, R., and Luporini, P. (1981). Membrane specializations in the ciliate *Euplotes crassus* at the site of interaction of the ampules with the plasma membrane. *Eur. J. Cell Biol.* 23, 280–285.

de Puytorac, P., Grain, J., and Rodrigues de Santa Rosa, M. (1976). A propos de l'ultrastructure corticale du cilié hypotriche *Stylonychia mytilus* Ehrbg., 1838: les caracteristiques du cortex buccal adoral et paroral des Polyhymenophora Jankowski, 1967. *Trans. Am. Microsc. Soc.* 95, 327–345. doi: 10.2307/3225124

Didier, P., and Dragescjo, J. (1979). Organisation ultrastructurale du cortex de *Phaconidium metchnicoffi* (Cilié Hétérotriche). *Protistologica* 15, 33–42.

Dong, J., Chen, X., Liu, Y., Ni, B., Fan, X., and Li, L. (2020a). An integrative investigation of *Parabistichella variabilis* (Protista, Ciliophora, Hypotrichia) including its general morphology, ultrastructure, ontogenesis, and molecular phylogeny. *J. Eukaryot. Microbiol.* 0, 1–17. doi: 10.1111/jeu.12809

Dong, J., Li, L., Fan, X., Ma, H., and Warren, A. (2020b). Two *Urosoma* species (Ciliophora, Hypotrichia): a multidisciplinary approach provides new insights into their ultrastructure and taxonomy. *Eur. J. Protistol.* 72:125661. doi: 10.1016/j.ejop.2019.125661

El-Serehy, H. A., Aboulela, H., Al-Misned, F., Kaiser, M., Al-Rasheid, K., and El-Din, H. E. (2012). Heavy metals contamination of a Mediterranean coastal ecosystem, eastern Nile Delta, Egypt. *Turk. J. Fish. Aquat. Sci.* 12, 751–760. doi: 10.4194/1303-2712-v12_4_03

Fauré-Fremiet, E., and André, J. (1968). Fine structure of *Euplotes eurystomus* (Wrz). *Arch. Anat. Microsc. Morphol. Exp.* 57, 53–78.

Fischer-Defoy, D., and Hausmann, K. (1981). Microtubules, microfilaments, and membranes in phagocytosis: structure and function of the oral apparatus of the ciliate *Climacostomum virens*. *Differentiation* 20, 141–151. doi: 10.1111/j.1432-0436.1981.tb01168.x

Foissner, W. (1978). *Euplotes moebiusi* f. *quadricirratus* (Ciliophora, Hypotrichida) I. Die feinstruktur des cortex und der argyrophilen strukturen. Arch. Protistenk. 120, 86–117. doi: 10.1016/S0003-9365(78)80014-1

Foissner, W. (1984). Taxonomie und ökologie einiger ciliaten (Protozoa, Ciliophora) des saprobiensystems. I: genera litonotus, amphileptus, opisthodon. *Hydrobiologia* 119, 193–208. doi: 10.1007/BF00015210

Foissner, W., and Al-Rasheid, K. (2006). A unified organization of the stichotrichine oral apparatus, including a description of the buccal seal (Ciliophora: Spirotrichea). *Acta Protozool.* 45, 1–16. doi: 10.11646/zootaxa.504.1.1

Foissner, W., Jung, J. H., Filker, S., Rudolph, J., and Stoeck, T. (2014). Morphology, ontogenesis and molecular phylogeny of *Platynematum salinarum* nov. spec., a new scuticociliate (Ciliophora, Scuticociliatia) from a solar saltern. *Eur. J. Protistol.* 50, 174–184. doi: 10.1016/j.ejop.2013.10.001

Fukang, G., and Lingmei, J. (1996). An ultrastructural study on cortex and macronucleus of *Euplotes encysticus*. *Zool. Res.* 17, 16–22. (in Chinese with English summary).

Gao, F., Huang, J., Zhao, Y., Li, L., Liu, W., Miao, M., et al. (2017). Systematic studies on ciliates (Alveolata, Ciliophora) in China: progress and achievements based on molecular information. *Eur. J. Protistol.* 61, 409–423. doi: 10.1016/j.ejop.2017.04.009

Gao, F., Warren, A., Zhang, Q., Gong, J., Miao, M., Sun, P., et al. (2016). The all-data-based evolutionary hypothesis of ciliated protists with a revised classification of the phylum Ciliophora (Eukaryota, Alveolata). *Sci. Rep.* 6:24874. doi: 10.1038/srep24874

Gliddon, R. (1966). Ciliary organelles and associated fibre systems in *Euplotes eurystomus* (Ciliata, Hypotrichida): I. Fine structure. *J. Cell Sci.* 1, 439–448.

Gong, Z., Fan, X., Ma, R., and Ni, B. (2018). Ultrastructure of vegetative cells and resting cysts, and live observations of the encystation and excystation processes in *Diophrys oligothrix* Borror, 1965 (Protista, Ciliophora). *J. Morphol.* 279, 1397–1407. doi: 10.1002/jmor.20851

Görtz, H. D. (1982). Discharge of cortical ampules in *Euplotes aediculatus* Pierson, 1943 (Ciliophora, Hypotrichida). *Arch. Protistenk.* 125, 31–40. doi: 10.1016/s0003-9365(82)80003-1

Grim, J. N. (1967). Ultrastructure of pellicular and ciliary structures of *Euplotes eurystomus*. *J. Protozool.* 14, 625–633. doi: 10.1111/j.1550-7408.1967.tb02052.x

Grim, J. N. (1972). Fine structure of the surface and infraciliature of *Gastrostyla steinii*. *J. Eukaryot. Microbiol.* 19, 113–126. doi: 10.1111/j.1550-7408.1972.tb03424.x

Grim, J. N., Halcrow, K. R., and Harshbarger, R. D. (1980). Microtubules beneath the pellicles of two ciliate protozoa as seen with the SEM. *J. Protozool.* 27, 308–310. doi: 10.1111/j.1550-7408.1980.tb04262.x

Grimes, G. W. (1972). Cortical structure in nondividing and cortical morphogenesis in dividing *Oxytricha fallax*. *J. Protozool.* 19, 428–445. doi: 10.1111/j.1550-7408.1972.tb03498.x

Grimes, G. W., and L'hernault, S. W. (1978). The structure and morphogenesis of the ventral ciliature in *Paraurostyla hymenophora*. *J. Protozool.* 25, 65–74. doi: 10.1111/j.1550-7408.1978.tb03869.x

Gu, F., Chen, L., Ni, B., and Zhang, X. (2002). A comparative study on the electron microscopic enzymo-cytochemistry of *Paramecium bursaria* from light and dark cultures. *Eur. J. Protistol.* 38, 267–278. doi: 10.1078/0932-4739-00875

Gu, F., and Ni, B. (1993). The exploration of preparing protozoan specimen for scanning electron microscopy. *J. Chin. Electron Microsc. Soc.* 12, 525–529.

Gu, F., and Ni, B. (1995). An ultrastructural study on resting cyst of *Euplotes encysticus*. *Acta Biol. Exp. Sin.* 28, 163–171.

Gupta, R., Abraham, J. S., Sripoorna, S., Maurya, S., Toteja, R., Makhija, S., et al. (2020). Description of a new species of *Tetmemena* (Ciliophora, Oxytrichidae) using classical and molecular markers. *J. King Saud Univ. Sci.* 32, 2316–2328. doi: 10.1016/j.jksus.2020.03.009

Hausmann, K. (1978). Extrusive organelles in protists. *Int. Rev. Cytol.* 52, 197–276. doi: 10.1016/s0074-7696(08)60757-3

Hausmann, K., and Bradbury, P. C. (1996). *Ciliates: Cells as Organisms*. Heidelberg: Spektrum Akademischer Verlag.

Hausmann, K., and Kaiser, J. (1979). Arrangement and structure of plates in the cortical alveoli of the hypotrich ciliate, *Euplotes vannus*. *J. Ultrastruct. Res.* 67, 15–22. doi: 10.1016/S0022-5320(79)80013-1

Hill, B. F. (1990). *Uronychia transfuga* (O. F. Müller, 1786) Stein, 1859 (Ciliophora, Hypotrichia, Uronychiidae): cortical structure and morphogenesis during division. *J. Protozool.* 37, 99–107. doi: 10.1111/j.1550-7408.1990.tb05877.x

Hofmann, A. H., and Bardele, C. F. (1987). Stomatogenesis in cyrtophorid ciliates: *Trithigmostoma steini* (Blochmann, 1895): from somatic Kkineties to Oral Kineties. *Eur. J. Protistol.* 23, 2–17. doi: 10.1016/s0932-4739(87)80003-2

Hu, X., Lin, X., and Song, W. (2019). *Ciliate Atlas: Species Found in the South China Sea*. Beijing: Science Press.

Huang, J. B., Zhang, T., Zhang, Q., Li, Y., Warren, A., Pan, H., et al. (2018). Further insights into the highly derived haptorids (Ciliophora, Litostomatea): Phylogeny based on multigene data. *Zool. Scr.* 47, 231–242. doi: 10.1111/zsc.12269

Jerka-Dziadosz, M., Dosche, C., Kuhlmann, H. W., and Heckmann, K. (1987). Signal-induced reorganization of the microtubular cytoskeleton in the ciliated protozoon *Euplotes octocarinatus*. *J. Cell Sci.* 87, 555–564.

Jerka-Dziadosz, M., and Wiernicka, L. (1992). Ultrastructural studies on the development of cortical structures in the ciliary pattern mutants of the hypotrich ciliate *Paraurostyla weissei*. *Eur. J. Protistol.* 28, 258–272. doi: 10.1016/s0932-4739(11)80232-4

Kchaou, N., Elloumi, J., Drira, Z., Hamza, A., Ayadi, H., Bouain, A., et al. (2009). Distribution of ciliates in relation to environmental factors along the coastline of the Gulf of Gabes, Tunisia. *Estuarine Coastal Shelf Sci.* 83, 414–424. doi: 10.1016/j.ecss.2009.04.019

Kim, S. J., and Min, G. S. (2011). First record of three *Uronychia* species (Ciliophora: Spirotrichea: Euplotida) from Korea. *Korean J. Syst. Zool.* 27, 25–33. doi: 10.5635/kjsz.2011.27.1.025

Kloetzel, J. A. (1974). Feeding in ciliated protozoa: i. Pharyngeal disks in Euplotes: a source of membrane for food vacuole formation. *J. Cell Sci.* 15, 379–401.

Kloetzel, J. A. (1991). Identification and properties of plateins, major proteins in the cortical alveolar plates of Euplotes. *J. Protozool.* 38, 392–401. doi: 10.1111/j.1550-7408.1991.tb01376.x

Küppers, G. C. (2020). A new species of *Uronychia* (Spirotrichea: Euplotida) from Argentina. *Eur. J. Protistol.* 75:125706. doi: 10.1016/j.ejop.2020.125706

Kurth, T., and Bardele, C. F. (2001). Fine structure of the cyrtophorid ciliate *Chlamydodon mnemosyne* Ehrenberg, 1837. *Acta Protozool.* 40, 33–48. doi: 10.1016/S0378-1097(00)00560-7

Lenzi, P., and Rosati, G. (1993). Ultrastructural study of *Euplotidium itoi* (Ciliata Hypotrichida). *Eur. J. Protistol.* 29, 453–461. doi: 10.1016/S0932-4739(11)80408-6

Leonildi, A., Erra, F., Banchetti, R., and Ricci, N. (1998). The ethograms of *Uronychia transfuga* and *Uronychia setigera* (Ciliata, Hypotrichida): a comparative approach for new insights into the behaviour of protozoa. *Eur. J. Protistol.* 34, 426–435. doi: 10.1016/s0932-4739(98)80011-4

Li, Y., Chen, X., Wu, K., Pan, J., Long, H., and Yan, Y. (2020). Characterization of simple sequence repeats (SSRs) in ciliated protists inferred by comparative genomics. *Microorganisms* 8:662. doi: 10.3390/microorganisms8050662

Lian, C., Luo, X., Warren, A., Zhao, Y., and Jiang, J. (2020). Morphology and phylogeny of four marine or brackish water spirotrich ciliates (Protozoa, Ciliophora) from China, with descriptions of two new species. *Eur. J. Protistol.* 72:125663. doi: 10.1016/j.ejop.2019.125663

Lobban, C. S., Modeo, L., Verni, F., and Rosati, G. (2005). *Euplotes uncinatus* (Ciliophora, Hypotrichia), a new species with zooxanthellae. *Mar. Biol.* 147, 1055–1061. doi: 10.1007/s00227-005-0024-3

Lynn, D. H. (1976). Comparative ultrastructure and systematics of the Colpodida. Structural conservatism hypothesis and a description of Colpoda steinii Maupas. *J. Protozool.* 23, 302–314. doi: 10.1111/j.1550-7408.1976.tb03776.x

Lynn, D. H. (1981). The organization and evolution of microtubular organelles in ciliated protozoa. *Biol. Rev.* 56, 243–292. doi: 10.1111/j.1469-185X.1981.tb00350.x

Lynn, D. H. (2008). *The Ciliated Protozoa: Characterization, Classification, and Guide to the Literature*. Dordrecht: Springer.

Ma, H., Li, J., Warren, A., Ba, S., and Lu, X. (2019). Morphogenesis of the Euplotid ciliate *Uronychia binucleata* Young, 1922 (Ciliophora, Hypotrichia). *J. Ocean Univ. China* 18, 467–473. doi: 10.1007/s11802-019-3956-9

Mendez-Sanchez, D., Mayen-Estrada, R., and Hu, X. (2020). Euplotes octocarinatus Carter, 1972 (Ciliophora, Spirotrichea, Euplotidae): considerations on its morphology, phylogeny, and biogeography. *Eur. J. Protistol.* 74:125667. doi: 10.1016/j.ejop.2019.125667

Morelli, A., Giambelluca, A., Lenzi, P., Rosati, G., and Verni, F. (1996). Ultrastructural features of the peculiar filter-feeding hypotrich ciliate *Uronychia transfuga*. *Micron* 27, 399–406. doi: 10.1016/s0968-4328(96)00027-3

Pitelka, D. R. (1965). New observations on cortical ultrastructure in *Paramecium*. *J. Microsc. (Paris)* 4, 373–394.

Randall, J. T., and Jackson, S. F. (1958). Fine structure and function in *Stentor polymorphus*. *J. Cell Biol.* 4, 807–830. doi: 10.1083/jcb.4.6.807

Rosati, G., and Modeo, L. (2003). Extrusomes in ciliates: diversification, distribution, and phylogenetic implications. *J. Eukaryot. Microbiol.* 50, 383–402. doi: 10.1111/j.1550-7408.2003.tb00260.x

Rosati, G., Verni, F., Bracchi, P., and Dini, F. (1987). An ultrastructural analysis of the ciliated protozoon *Aspidisca* sp. *Trans. Am. Microsc. Soc.* 106, 31–52. doi: 10.2307/3226282

Rosati, R. G. (1970). Fine structure of *Diophrys scutum* (Dujardin). *Arch. Anat. Microsc. Morphol. Exp.* 59, 221–234.

Ruffolo, J. J. (1976). Fine structure of the dorsal bristle complex and pellicle of *Euplotes*. *J. Morphol.* 148, 469–487. doi: 10.1002/jmor.1051480405

Sandborn, E., Koen, P. F., McNabb, J. D., and Moore, G. (1964). Cytoplasmic microtubules in mammalian cells. *J. Ultrastruct. Res.* 11, 123–138. doi: 10.1016/S0022-5320(64)80097-6

Schmidt, S. L., Foissner, W., Schlegel, M., and Bernhard, D. (2007). Molecular phylogeny of the Heterotrichea (Ciliophora, Postciliodesmatophora) based on small subunit rRNA gene sequences. *J. Eukaryot. Microbiol.* 54, 358–363. doi: 10.1111/j.1550-7408.2007.00269.x

Schwarz, M. V. J., Zuendorf, A., and Stoeck, T. (2007). Morphology, ultrastructure, molecular phylogeny, and autecology of *Euplotes elegans* Kahl, 1932 (Hypotrichida; Euplotidae) isolated from the anoxic Mariager Fjord, Denmark. *J. Eukaryot. Microbiol.* 54, 125–136. doi: 10.1111/j.1550-7408.2007.00243.x

Shen, Z., Shao, C., Gao, S., Lin, X., Li, J., Hu, X., et al. (2009). Description of the rare marine ciliate, *Uronychia multicirrus* song, 1997 (Ciliophora; Euplotida) based on morphology, morphogenesis and SS rRNA gene sequence. *J. Eukaryot. Microbiol.* 56, 296–304. doi: 10.1111/j.1550-7408.2009.00409.x

Sheng, Y., Duan, L., Cheng, T., Qiao, Y., Stover, N. A., and Gao, S. (2020). The completed macronuclear genome of a model ciliate *Tetrahymena thermophila* and its application in genome scrambling and copy number analyses. *Sci. China: Life Sci.* 63, 1534–1542. doi: 10.1007/s11427-020-1689-4

Sheng, Y., He, M., Zhao, F., Shao, C., and Miao, M. (2018). Phylogenetic relationship analyses of complicated class Spirotrichea based on transcriptomes from three diverse microbial eukaryotes: *Uroleptopsis citrina*, *Euplotes vannus* and *Protocruzia tuzeti*. *Mol. Phylogenet. Evol.* 129, 338–345. doi: 10.1016/j.ympev.2018.06.025

Shi, X., Liu, G., Wang, C., and Hu, X. (2017). Description of a new brackish water ciliate, *Uronychia xinjiangensis* n. sp. (Ciliophora, Euplotida) based on morphology, morphogenesis and molecular phylogeny. *Acta Protozool.* 56, 303–315. doi: 10.4467/16890027AP.17.026.7828

Song, W. (1997). On the morphology and infraciliature of a new marine hypotrichous ciliate, *Uronychia multicirrus* sp. n. (Ciliophora: Hypotrichida). *Acta Protozool.* 4, 279–285.

Song, W., and Shao, C. (2017). *Ontogenetic Patterns of Hypotrich Ciliates*. Beijing: Science Press.

Song, W., Warren, A., and Hu, X. (2009). *Free-Living Ciliates in the Bohai and Yellow Seas, China*. Beijing: Science Press.

Song, W., and Wilbert, N. (1997). Morphological investigations on some free living ciliates (Protozoa, Ciliophora) from China sea with description of a new hypotrichous genus, *Hemigastrostyla* nov. gen. *Arch. Protistenk.* 148, 413–444. doi: 10.1016/s0003-9365(97)80020-6

Song, W., Wilbert, N., Chen, Z., and Shi, X. (2004). Considerations on the systematic position of *Uronychia* and related euplotids based on the data of ontogeny and 18S rRNA gene sequence analyses, with morphogenetic redescription of *Uronychia setigera* Calkins, 1902 (Cilio-phora: Euplotida). *Acta Protozool.* 43, 313–328.

Sun, J. J., Ren, Z. H., Fan, X., Ni, B., and Gu, F. (2018). Ultrastructural study on the kinetosomes and associated microtubules of adoral membranelles and marginal cirri of *Pseudourostyla cristata*. *J. Chin. Electron Microsc. Soc.* 37, 289–297. doi: 10.3969/j.issn.1000-6281.2018.03.014

Valbonesi, A., and Luporini, P. (1990). A new species of *Uronychia* (Ciliophora, Hypotrichida) from Antarctica: *Uronychia antarctica*. *Boll. Zool.* 57, 365–368. doi: 10.1080/11250009009355721

Vďačný, P., and Rajter, L. (2015). Reconciling morphological and molecular classification of predatory ciliates: evolutionary taxonomy of dileptids (Ciliophora, Litostomatea, Rhynchostomatia). *Mol. Phylogenet. Evol.* 90, 112–128. doi: 10.1016/j.ympev.2015.04.023

Verni, F., and Gualtieri, P. (1997). Feeding behaviour in ciliated protists. *Micron* 28, 487–504. doi: 10.1016/s0968-4328(97)00028-0

Verni, F., Rosati, G., and Luporini, P. (1978). Preconjugant cell-cell interaction in the ciliate *Euplotes crassus*: a possible role of the ciliary ampules. *J. Exp. Zool.* 204, 171–179. doi: 10.1002/jez.1402040205

Wang, C., Zhang, T., Wang, Y., Katz, L. A., Gao, F., and Song, W. (2017). Disentangling sources of variation in SSU rDNA sequences from single cell analyses of ciliates: impact of copy number variation and experimental error. *Proc. R. Soc. B.* 284:20170425. doi: 10.1098/rspb.2017.0425

Wang, Y., Wang, C., Jiang, Y., Katz, L. A., Gao, F., and Yan, Y. (2019). Further analyses of variation of ribosome DNA copy number and polymorphism in ciliates provide insights relevant to studies of both molecular ecology and phylogeny. *Sci. China Life Sci.* 62, 203–214. doi: 10.1007/s11427-018-9422-5

Warren, A., Patterson, D. J., Dunthorn, M., Clamp, J. C., Achilles-Day, U. E. M., Aescht, E., et al. (2017). Beyond the "Code": a guide to the description and documentation of biodiversity in ciliated protists (Alveolata, Ciliophora). *J. Eukaryot. Microbiol.* 64, 539–554. doi: 10.1111/jeu.12391

Wicklow, B. J. (1983). Ultrastructure and cortical morphogenesis in the euplotine hypotrich *Certesia quadrinucleata* Fabre-Domergue, 1885 (Ciliophora, Protozoa). *J. Eukaryot. Microbiol.* 30, 256–266. doi: 10.1111/j.1550-7408.1983.tb02912.x

Wilbert, N. (1975). Eine verbesserte Technik der Protargolimprägnation für Ciliaten. *Mikrokosmos* 64, 171–179.

Wilbert, N., and Kahan, D. (1981). Ciliates of solar lake on the red sea shore. *Arch. Protistenk.* 124, 70–95. doi: 10.1016/s0003-9365(81)80004-8

Wirnsberger, E., and Hausmann, K. (1988). Fine structure of *Pseudokeronopsis carnea* (Ciliophora, Hypotrichida). *J. Eukaryot. Microbiol.* 35, 182–189. doi: 10.1111/j.1550-7408.1988.tb04321.x

Wu, T., Li, Y., Lu, B., Shen, Z., Song, W., and Warren, A. (2020). Morphology, taxonomy and molecular phylogeny of three marine peritrich ciliates, including two new species: *Zoothamnium apoarbuscula* n. sp. and *Z. apohentscheli* n. sp. (Protozoa, Ciliophora, Peritrichia). *Mar. Life Sci. Technol.* 2, 334–348. doi: 10.1007/s42995-020-00046-y

Yan, Y., Maurer-Alcalá, X. X., Knight, R., Pond, S. L. K., and Katz, L. A. (2019). Single-cell transcriptomics reveal a correlation between genome architecture and gene family evolution in ciliates. *Mbio* 10: e002524-19.

Conflict of Interest: The authors declare that the research was conducted in the absence of any commercial or financial relationships that could be construed as a potential conflict of interest.